RISM-Assisted Analysis of the Role of Alkali Metal Hydroxides in the Solvation of Cellulose in Alkali/urea Aqueous Solutions

Eugene Huh
Yonsei University
Ji-Hyun Yang
Yonsei University
Chang-Ha Lee
Yonsei University
Ik-sung Ahn (iahn@yonsei.ac.kr)
Yonsei University https://orcid.org/0000-0002-1347-2037
Byung Jin Mhin
Paichai University: Pai Chai University

Research Article

Keywords: Cellulose, reference interaction site model (RISM), Kirkwood-Buff integral (KBI), alkali metal hydroxide, urea

Posted Date: May 10th, 2021

DOI: https://doi.org/10.21203/rs.3.rs-425463/v1

Version of Record: A version of this preprint was published at Cellulose on October 27th, 2021. See the published version at https://doi.org/10.1007/s10570-021-04214-w.

RISM-assisted analysis of the role of alkali metal hydroxides in the solvation of cellulose in alkali/urea aqueous solutions

Eugene Huh[†], Ji-Hyun Yang[†], Chang-Ha Lee[†], Ik-Sung Ahn[*, †], Byung Jin Mhin[*,‡]

[†]*Department of Chemical and Biomolecular Engineering, Yonsei University, Seoul 120-749, South Korea*

[‡]*Department of Chemistry, Paichai University, Daejeon 302-735, South Korea*

*Corresponding authors
Tel.: +(82) 2-2123-2752, +(82) 42-520-5611

Eugene Huh: eugeneh55@gmail.com
Ji-Hyun Yang: prji17@naver.com
Chang-Ha Lee: leech@yonsei.ac.kr ORCID 0000-0001-8769-7936
Ik-Sung Ahn*: iahn@yonsei.ac.kr ORCID 0000-0002-1347-2037
Byung Jin Mhin*: mhin@pcu.ac.kr

The three-dimensional reference interaction site model theory with the Kovalenko-Hirata closure (3D-RISM-KH) combined with the Kirkwood-Buff integral (KBI) was used to clarify the role of alkali metal hydroxides (MOHs) in cellulose solvation in alkali/urea aqueous solutions. The KBI and excess number of MOHs showed that their access and affinity to cellulose were both in the order LiOH > NaOH > KOH. The cavity and interaction volumes for cellulose indicate that the alkali metal ions closer in proximity to cellulose induce thermal fluctuations of cellulose molecules more easily and cause more electrostatic interactions and hydrogen bonding with cellulose. These calculation results support the hypothesis of cellulose charging up, which claims that cellulose-ion interactions cause cellulose solvation. The energy and chemical potential of cellulose solvation confirmed the affinity and interaction of MOHs with cellulose. Solvent reorganization, whose energy primarily determined the solvation energy, was found to be facilitated by the more proximal MOH when in the presence of urea. 3D-RISM-KH combined with KBI produced quantitative information regarding the distribution and attractive interaction of MOHs (especially LiOH) with cellulose, which clarified their role in cellulose solvation in alkali/urea aqueous solutions.

Keywords: Cellulose, reference interaction site model (RISM), Kirkwood-Buff integral (KBI), alkali metal hydroxide, urea

36

Introduction

Recently, aqueous solutions of urea and various kinds of alkali metal hydroxides (e.g., LiOH, NaOH, and KOH) have shown different solvation capabilities toward cellulose molecules of varying molecular weights (Cai and Zhang 2005; Wang et al. 2017). Three cellulose molecules with viscosity-average molecular weights of 4.5 × 104, 11.5 × 104 and 37.2 × 104 were found to be soluble in a 4.2 % (w/w) LiOH/12 % (w/w) urea solution precooled to -10°C (Cai and Zhang 2005). A 7 % (w/w) NaOH/12 % (w/w) urea solution could dissolve the first two cellulose molecules, while a 9.8 % (w/w) KOH/12 % (w/w) urea solution did not dissolve any of the tested cellulose molecules. Using differential scanning calorimetry analysis, Wang et al. (Wang et al. 2017) estimated cellulose solvation to be feasible at approximately -5°C in LiOH/urea solutions but at -20°C in NaOH/urea solutions. By measuring pulsed field-gradient spin-echo NMR intensities, they calculated that the ratios of Li^+ and Na^+ bound to cellulose were 14.3 % and 4.8 %, respectively. These experimental results indicate that these ions' interaction with cellulose and contribution to cellulose solvation are in the order $Li^+ > Na^+ > K^+$. The results of a molecular dynamics (MD) simulation suggest that the interaction between cellulose and alkali metal hydroxides such as LiOH and NaOH is primarily an electrostatic interaction. In their calculation, Li^+ ions were closer in proximity to cellulose than Na^+ ions, and the average distance of Li^+ from the oxygens of cellulose was smaller than that of Na^+. The probability of finding Li^+ ions within the same distance of cellulose was higher than that of finding Na^+ ions (Wang et al. 2017). Xiong et al. (Xiong et al. 2013) investigated the dissolution of cellobiose, a unit of cellulose, in alkali solutions to clarify the role of alkali metal ions in cellulose solvation. In the ^{13}C-NMR spectroscopy of cellobiose, a larger downfield chemical shift and shorter ^{13}C relaxation time were detected in the order LiOH > NaOH > KOH. This means that the interaction between cellobiose and alkali metal ions is on the same order, which is consistent with the contribution of alkali metal ions to cellulose solvation (Xiong et al. 2013).

In our previous work (Huh et al. 2020), the three-dimensional reference interaction site model theory with the Kovalenko-Hirata closure (3D-RISM-KH) was applied to calculate the solvation energy of cellulose in NaOH/urea aqueous solution at 261 K and to determine the contribution of each solvent species (i.e.,

Na^+, OH^-, urea, and water) to cellulose solvation. Water molecules were found to be located nearer to cellulose in NaOH/urea aqueous solutions than in NaOH solutions without urea. As a result, the inclusion of urea caused a reduction in the solvent reorganization energy of cellulose from 163 to –1,198 kcal/mole and a decrease in the interaction energy between cellulose and the solvent by more than 100 kcal/mole.

In this work, a system for cellulose solvation was extended to aqueous solutions of urea and various alkali metal hydroxides, such as LiOH, NaOH, and KOH. The objective of this work is to determine the role of alkali metal hydroxides in cellulose solvation (i.e., their affinity to cellulose) by calculating and comparing the distribution of the solvent species and the partial molar volume and solvation energy of cellulose. For this purpose, 3D-RISM-KH (Gusarov et al. 2012; Kovalenko 2013, 2017; Kovalenko and Gusarov 2018) combined with the Kirkwood-Buff integral (KBI) (Giambaşu et al. 2015; Giambaşu et al. 2014; Krüger et al. 2013) was used in this study.

Methods

The KBI, G_γ is defined as the spatial integral over the pair distribution function ($g_\gamma^{uv}(r)$):

$$G_\gamma = \int_V [g_\gamma^{uv}(r) - 1] dr \quad (1)$$

where superscripts u and v denote the solute and solvent, respectively; V is the system volume over which the integration is carried out; and r is the distance between the solute and the solvent species. $g_\gamma^{uv}(r)$ is the ratio of the probability of finding the solvent species γ at r, which is determined from the 3D-RISM calculations, to the probability of finding γ in the bulk solvent phase. The unit of G_γ is the volume per single solute molecule (Å^3/molecule). G_γ indicates the accessibility of γ to the solute, which is correlated with the affinity of γ to the solute (Nicol et al. 2017; Wernersson et al. 2015). The KBI has been considered appropriate for describing all types of intermolecular interactions necessary for determining the thermodynamic properties of a solution. For example, it has been used to calculate the excess number of γ around the single solute molecule, N_γ^{excess} as follows (Shimizu 2004; Shimizu et al. 2013):

$$N_\gamma^{excess} = \rho_\gamma (G_\gamma + V_C) \quad (2)$$

where ρ_γ is the number density of γ and V_C is the excluded volume of the solute. The sum of G_γ and V_C corresponds to the real volume in which γ can exist near the solute. The excess numbers of various solvent species allow us to compare their interaction with the solute.

The partial molar volume of the solute, $\bar{V}$, is also affected by its interaction with the solvent species and is defined as follows (Chalikian and Breslauer 1996; Imai 2007a; Imai et al. 2007b; Patel et al. 2011):

$$\bar{V} = V_C + V_I + V_{id} \quad (3)$$

where V_I and V_{id} denote the interaction volume and the ideal fluctuation volume, respectively. V_{id} is caused by the translational degrees of freedom of the solvent (Imai 2007a). V_C, which is also called the cavity volume, consists of the region occupied by the solute (V_M, the geometric volume) and an empty border region between the solute and the unaltered, uniform pure solvent (V_T, the thermal volume) (Lee 1983; Patel et al. 2011). V_T results from thermally induced molecular fluctuations between the solute and solvent species (Chalikian and Breslauer 1996; Imai 2007a) and may simply be considered the void volume due to their imperfect packing (Imai 2007a). V_I represents the change in the solvent volume due to the intermolecular electrostatic interaction and hydrogen bonding between cellulose and solvent species (Chalikian and Breslauer 1996). In this study, the more nonpolar and polar interaction of cellulose with the solvent will cause smaller V_T (i.e., V_C) and V_I, respectively, which will lead to a smaller $\bar{V}$.

The solvation energy (ΔE) and solvation entropy ($T\Delta S$), which are needed for calculating the excess chemical potential ($\Delta\mu$), are defined as the sum of solute-solvent interaction (uv) and solvent-solvent reorganization (R) terms:

$$\Delta E = E^{uv} + \Delta E^R \quad (4)$$

$$T\Delta S = T\Delta S^{uv} + T\Delta S^R = T\Delta S^{uv} + \Delta E^R \quad (5)$$

As ΔE^R and $T\Delta S^R$ result from the change in the solvent-solvent interaction upon insertion of the solute molecule (Ben-Naim 1978; Gallicchio et al. 2000; Lazaridis 2000; Misin 2017), they have the same values. Then

$$\Delta\mu = \Delta E - T\Delta S = E^{uv} - T\Delta S^{uv} \quad (6)$$

3D-RISM is known to strongly overestimate the excess chemical potential (Misin 2017; Sergiievskyi et al. 2014). Sergiievskyi et al. (Sergiievskyi et al. 2014) showed that this is primarily caused by a high solvent pressure, which leads to

overestimation of the solute insertion work. Misin (Misin 2017) argued that water molecules near a large solute, such as cellulose, undergo substantial reorganization. The density of the water molecules immediately next to the solute is lower than that of bulk water molecules, which is caused by the lack of attractive interaction with the hydrophobic moiety of the solute. Instead, they are strongly drawn in by the bulk water, forming a strong tetrahedral network. These solvent reorganizations create large cavities near the hydrophobic moiety of the solute. Such a dewetting transition cannot be considered by conventional 3D-RISM and requires pressure correction of 3D-RISM (Misin 2017). $\Delta\mu_{PC+}$, or $\Delta\mu$ corrected by including the advanced pressure correction (PC+) and the partial molar volume of cellulose, is expressed as follows:

$$\Delta\mu_{PC+} = \Delta\mu + (P_{id} - P)\bar{V} \quad (7)$$

where P_{id} is an ideal gas pressure of the solvent given by $P_{id} = \rho_{Tot}k_BT$ and P is given by $P = \frac{1}{2}k_BT\left(\frac{1}{k_BT\chi_T} + N_{site}\rho_{Tot}\right)$. ρ_{Tot} and N_{site} are the number densities of all solvent species and the number of sites (atoms) in the solvent, respectively (Misin et al. 2016; Sergiievskyi et al. 2014).

The 3D-RISM-KH calculation and MD simulation were performed with the AMBER16 package (Case et al. 2010). As a model cellulose molecule, the molecule with the Iβ structure and degree of polymerization of 8 was selected in this study. The following eight solvents were tested for cellulose solvation at 261 K: LiOH/urea aqueous solution (abbreviated as solvent LU), NaOH/urea (solvent NU), KOH/urea (solvent KU), pure water (solvent WO), urea aqueous solution (solvent UO), LiOH solution (solvent LO), NaOH solution (solvent NO), and KOH solution (solvent KO). The latter 5 solvents were used for comparison with the first 3 solvents (LU, NU, and KU). For meaningful comparison of the cellulose solvation thermodynamics and solvent affinities toward cellulose, the number ratio of water, MOH, and urea was maintained at 27.75:1:1. The 3D-RISM-KH calculations were performed in a 32 x 40 x 72 $Å^3$ box with a spacing of 0.5 Å. TIP3P water was used as the solvent water. The detailed calculation method is described in Supplementary Information. The initial density and pressure values of each solvent are shown in Table S1 (see Supplementary Information). The force-field parameters and partial charge were assigned using the General Amber Force Field and AM1-BCC charge model, respectively (Jakalian et al. 2000; Jakalian et al. 2002). The structure of the model cellulose

molecule was created using a cellulose-builder (Gomes and Skaf 2012). The geometric volume (V_M) of cellulose was calculated using Protein Volume 1.3 (Chen and Makhatadze 2015).

Results and discussion

Affinity of Li^+, Na^+, and K^+ toward cellulose

Fig. 1 shows an example of the pair distribution functions used in Eq. (1). KBI (G_γ) values were calculated for all solvent species in the 8 different solvents and are shown in Fig. 2. The negative G_γ values arise due to the excluded volume (V_C) of cellulose (Sergiievskyi et al. 2014), and solvent species with a more negative G_γ have a lower probability of existing near cellulose and are less accessible to cellulose. The G_γ was found to be in the order urea >> LiOH > Water > NaOH > KOH. G_{urea} seems to be constant regardless of the other solvent species, such as MOHs, which corresponds well with the positioning of urea above and below the pyranose rings of cellulose and its interaction with cellulose independent of MOH (Huh et al. 2020; Wernersson et al. 2015; Xiong et al. 2013). G_{MOH} was found to be in the order LiOH > NaOH > KOH regardless of whether urea was present in the solvent. G_{LiOH} was higher than G_{water} in solvents LO and LU, while G_{NaOH} and G_{KOH} were lower than G_{water}. Li^+, Na^+, and K^+ have the same charge but different sizes, which were in the order Li^+ < Na^+ < K^+ (see Table S2 in Supplementary Information). Hence, Li^+ is most easily accessible to cellulose, which enables the strongest electrostatic interaction and corresponds well with the experimental finding that cellulose is most favorably soluble in solvent LU. Due to these differences in the electrostatic interaction of MOHs with cellulose, G_{water} in the solvent containing LiOH was the smallest, while that in the solvent containing KOH was the largest regardless of the presence of urea (see Fig. 1).

Table 1 summarizes the N_γ^{excess} of each solvent species in the 4 different solvents. The N_γ^{excess} values for cellulose in solvents WO, LO, NO, and KO are shown in Table S4. As expected from G_{MOH}, the smaller alkali metal ion yielded the larger N_{MOH}^{excess} (i.e., $N_{LiOH}^{excess} > N_{NaOH}^{excess} > N_{KOH}^{excess}$). The greater concentration close to cellulose implies a greater interaction between the corresponding metal ion and cellulose and a higher probability of making

cellulose into a polyelectrolyte in the order $Li^+ > Na^+ > K^+$. Hence, the N_{MOH}^{excess} data support the hypothesis of cellulose charging up (Nicol et al. 2017), which claims that cellulose-ion interactions can make cellulose into a polyelectrolyte and cause its solvation (Bialik et al. 2016).

As urea is positioned above and below the pyranose rings of cellulose, the region near cellulose that is available for water and MOHs decreases upon the addition of urea into the solvent. Hence, the difference between N_{MOH}^{excess} and N_{water}^{excess} is smaller when urea is present in the solvent. Due to the interaction with cellulose and the size of ion hydrates (see Table S2 in Supplementary Information), which is in the order $Li^+ > Na^+ > K^+$, N_{water}^{excess} was dependent on the kind of MOH: N_{water}^{excess} in solvent with LiOH < N_{water}^{excess} in solvent with NaOH < N_{water}^{excess} in solvent with KOH (see Table 1 and Fig. 3). Based on the G_γ and N_γ^{excess}, positioning of the solvent species around the single cellulose molecule is schematically depicted in Fig. 3. Note that MOHs and urea are capable of hydrophilic and hydrophobic interactions with cellulose, respectively (Huh et al. 2020).

Partial molar volume of cellulose dependent on alkali metal hydroxides

Cavity volume (V_C) and its component for each solvent species γ ($V_{C,\gamma}$) was calculated for cellulose in solvents LU, NU, and KU and is shown in Tables 2 and 3, respectively. The geometric volume (V_M), which is equal to the sum of the van der Waals volume (V_W) and void volume (V_V), was calculated to be 1173.3 Å^3, while V_W and V_V were 1061.7 Å^3 and 111.6 Å^3, respectively. Since V_M is constant regardless of the solvent, the difference in V_C for different solvents originates from the thermal volume (V_T). To further study the dependence of V_C on the kind of MOH, V_C was divided into three components: $V_{C,water}$, $V_{C,MOH}$, and $V_{C,urea}$. It was found in a previous study (Huh et al. 2020) that urea was predominantly positioned close to the hydrophobic part of cellulose (i.e., above and below the pyranose rings of cellulose), while MOH was positioned close to the hydrophilic part of cellulose (i.e., along the edges of cellulose). Hence, $V_{C,urea}$ was not affected by MOHs (see Table 3).

The radial distribution functions of Li^+, Na^+, and K^+ shown in Fig. 1 indicate the denser and more proximal distribution of Li^+ to cellulose than Na^+ and K^+. Hence, G_{MOH} and N_{MOH}^{excess} were in the order LiOH > NaOH > KOH. MOHs smaller and

nearer to cellulose are apt to more easily induce thermal fluctuation of cellulose molecules and to result in the further reduction of V_C, which leads to $V_{C,MOH}$ in the following order: $V_{C,LiOH} < V_{C,NaOH} < V_{C,KOH}$. The magnitudes of G_{water} and N_{water}^{excess} are in the order solvent LU < solvent NU < solvent KU; therefore, we see the opposite order for $V_{C,water}$: $V_{C,water}$ in solvent LU > $V_{C,water}$ in solvent NU > $V_{C,water}$ in solvent KU. The V_C values for cellulose in solvents LO, NO, and KO are shown in Table S5, while their water and MOH components are shown in Table S6. For the same MOH, $V_{C,water}$ is smaller in the presence of urea, which is consistent with the results of a previous study which indicated that water molecules were positioned closer in proximity to cellulose in the presence of urea (Huh et al. 2020).

Interaction volume (V_I) and its component for each solvent species γ ($V_{I,\gamma}$) was calculated for cellulose in solvents LU, NU, and KU and is shown in Tables 2 and 3, respectively. V_I was found to be in the order solvent LU (most negative) < solvent NU < solvent KU (least negative); these results imply that the most closely distributed LiOH (see Fig. 1) results in the most hydrophilic interaction with cellulose. When separately calculating $V_{I,water}$, $V_{I,MOH}$, and $V_{I,urea}$, the difference in V_I between the three solvents could not be explained with $V_{I,MOH}$. Even though G_{MOH} and N_{MOH}^{excess} were in the order LiOH > NaOH > KOH, the most negative $V_{I,MOH}$ caused by the most hydrophilic interaction between MOHs and cellulose was found in solvent KU. The most negative $V_{I,water}$ was found in solvent LU despite G_{water} and N_{water}^{excess} being in the order KOH > NaOH > LiOH. Therefore, MOHs might not be directly involved in the hydrophilic interaction with cellulose. Instead, a portion of the water molecules were positioned close to cellulose; for example, water molecules comprising ion hydrates might predominantly participate in electrostatic interactions and hydrogen bonding with cellulose, which explains the results for $V_{I,water}$ and $V_{I,MOH}$ in Table 3. The ideal fluctuation volume (V_{id}) was negligibly small compared to V_C and V_I (see Table 2), and its influence on $\bar{V}$ did not need to be considered. The V_I values for cellulose in solvents LO, NO, and KO are shown in Table S5, while their water and MOH components are shown in Table S6. Significant differences are not found in V_C and V_I, which implies that urea is indispensable for facilitating MOH-thermally-induced molecular fluctuations of

cellulose as well as causing water molecules in ion hydrates to participate in electrostatic interaction and hydrogen bonding with cellulose.

Thermodynamics of cellulose solvation depending on alkali metal hydroxides

The solvation energy and entropy of cellulose in solvents LU, NU, and KU are shown in Table 4, while those in solvents LO, NO, and KO are shown in Table S7. The superscripts uv and R denote that the corresponding energy terms consider solute-solvent interaction and solvent reorganization (i.e., solvent-solvent interaction), respectively. The solvation energy accounted for the experimental result of cellulose solvation (i.e., cellulose is most easily dissolved in solvent LU and not soluble in solvent KU).

The E^{uv} (direct solvation energy) in solvent LU is –481.4 kcal/mol and smaller than –470.9 and –450.7 kcal/mol in solvents NU and KU, respectively, which indicates that Li^+ is positioned closest to cellulose and experiences the strongest interaction with cellulose. Note that the difference in E^{uv} was affected more dominantly by MOHs than by water (compare the numbers in square and round brackets on the column for E^{uv} in Table 4). The following ΔE^{uv}_{MOH-WO} and ΔE^{uv}_{MOH-UO} were calculated to determine the effect of urea on the contribution of MOHs to E^{uv} (see Table 5):

$$\Delta E^{uv}_{MOH-WO} = E^{uv}\ (solvent\ \ LO, NO, KO) - E^{uv}(solvent\ \ WO) \quad (8)$$

$$\Delta E^{uv}_{MOH-UO} = E^{uv}\ (solvent\ \ LU, NU, KU) - E^{uv}(solvent\ \ UO) \quad (9)$$

As shown in Table 5, ΔE^{uv}_{MOH-UO} is much more negative than ΔE^{uv}_{MOH-WO}, and their difference is largest when the MOH is LiOH. Urea is believed to strengthen the interaction between cellulose and MOHs, especially LiOH. The $T\Delta S^{uv}$ in solvent LU is –518.7 kcal/mol and higher (i.e., less negative) than those in the other solvents, which indicates that the access of LiOH to cellulose is less hindered than the access of NaOH and KOH to cellulose.

Table 4 separately shows the contributions of water and MOHs to ΔE^R (see the numbers in round and square brackets on the column for ΔE^R). The reorganization of water and MOHs around cellulose is favored by type of MOH in the order LiOH > NaOH > KOH. The following $\Delta\Delta E^R_{MOH-WO}$ and $\Delta\Delta E^R_{MOH-UO}$ were calculated to determine the effect of urea on the contribution of MOHs to ΔE^R (see Table 5):

$$\Delta\Delta E^{R}_{MOH-WO} = \Delta E^{R}\ (solvent\ \ LO, NO, KO) - \Delta E^{R}\ (solvent\ \ WO) \quad (10)$$

$$\Delta\Delta E^{R}_{MOH-UO} = \Delta E^{R}\ (solvent\ \ LU, NU, KU) - \Delta E^{R}\ (solvent\ \ UO) \quad (11)$$

ΔE^{R} in the solvent containing urea is much smaller than that in the solvent without urea (compare Tables 4 and S6). Note that ΔE^{R} decreased by approximately 1300 kcal/mol in the presence of urea. As a result, $\Delta\Delta E^{R}_{MOH-UO}$ is much more negative than $\Delta\Delta E^{R}_{MOH-WO}$, and their difference is largest when MOH is LiOH. Hence, it is believed that urea induces the reorganization of water and MOHs, especially LiOH around cellulose, to favor solvent-solvent interactions. The chemical potentials of cellulose solvation were corrected by including advanced pressure correction (PC+) and are shown in Table 6 (see the column marked with $\Delta\mu_{PC+}$. The $\Delta\mu_{PC+}$ values are –193.8, –188.6, and –178.4 kcal/mol in solvents LU, NU, and KU, respectively, which agrees with the experimental result of cellulose solvation in these solvents. $\Delta\mu_{PC+}$ in the solvent without urea is shown in Table S8 and is higher (i.e., less negative) than that in the corresponding solvent with urea (e.g., –139.8 and –193.8 kcal/mol in solvents LO and LU, respectively). Note that the difference in $\Delta\mu_{PC+}$ between MOHs is not significant in the solvents without urea. The calculation results of E^{uv}, ΔE^{R}, and $\Delta\mu_{PC+}$ indicate that cellulose solvation in alkali/urea aqueous solutions was feasible due to the presence of urea in the solvent, and the contribution of MOHs was in the order LiOH > NaOH > KOH.

Conclusions

Alkali metal hydroxides (MOHs) in aqueous urea solutions were reported to favor cellulose solvation in the order LiOH > NaOH > KOH, as determined from the molecular weights of soluble cellulose and solvation temperatures. The three-dimensional reference interaction site model theory with the Kovalenko-Hirata closure (3D-RISM-KH) combined with the Kirkwood-Buff integral (KBI) was used in this study to determine the role of MOHs in cellulose solvation. For this purpose, the access and interaction of MOHs with cellulose was estimated by calculating the KBI and excess number of solvent species around cellulose, the partial molar volume of cellulose, and the thermodynamics of cellulose solvation. The KBI and excess number of MOHs were in the order LiOH > NaOH > KOH, which indicates the positioning of LiOH (i.e., Li^{+}) closest to cellulose and implies the strongest electrostatic interaction. The KBI of urea was much higher than that

of water, which agrees with the finding that urea prefers to be positioned near the hydrophobic surface of cellulose and is involved in hydrophobic interactions with cellulose independent of MOHs. The excess numbers of MOHs on the order of $N_{LiOH}^{excess} > N_{NaOH}^{excess} > N_{KOH}^{excess}$ supports the hypothesis of cellulose charging up, which claims that cellulose-ion interactions can turn cellulose into a polyelectrolyte and cause its solvation. The cavity and interaction volumes of cellulose, which are the dominant components of the partial molar volume of cellulose, were in the order of LiOH < NaOH < KOH, especially in the presence of urea. It is believed that the alkali metal ion nearer to cellulose induces thermal fluctuation of cellulose molecules more easily, and its hydrate causes more electrostatic interactions and hydrogen bonding with cellulose. The calculation results of E^{uv} and ΔE^{R} indicate that urea strengthens not only the interaction between cellulose and MOHs but also the solvent-solvent interaction, especially LiOH. The chemical potential of cellulose solvation was corrected by including the advanced pressure correction and shows that the contribution of MOHs to cellulose solvation was in the order LiOH > NaOH > KOH, especially when urea was present in the solvent. 3D-RISM-KH combined with KBI produced quantitative information regarding the distribution and interaction of MOHs with cellulose, clarified the role of MOHs, especially LiOH, in cellulose solvation, and helped explain the preferential dissolution of cellulose in LiOH/urea aqueous solutions.

Declarations

Ethical approval

This article does not contain any studies with human participants or animals performed by any of the authors.

Conflict of interest

The authors declare that they have no known competing financial interests or personal relationships that could have appeared to influence the work reported in this paper.

Acknowledgment

This work was supported by Yonsei University and PaiChai University research grants in 2020.

References

Ben-Naim A (1978) Standard thermodynamics of transfer. Uses and misuses J Phys Chem 82:792-803

Bialik E, Stenqvist B, Fang Y, Östlund Å, Furo I, Lindman BR, Lund M, Bernin D (2016) Ionization of cellobiose in aqueous alkali and the mechanism of cellulose dissolution J Phys Chem Lett 7:5044-5048

Cai J, Zhang L (2005) Rapid dissolution of cellulose in LiOH/urea and NaOH/urea aqueous solutions Macromol Biosci 5:539-548

Case D, Betz R, Cerutti D, Cheatham T, Darden T, Duke R AMBER16, 2016 San Francisco

Chalikian TV, Breslauer KJ (1996) On volume changes accompanying conformational transitions of biopolymers Biopolymers 39:619-626

Chen CR, Makhatadze GI (2015) ProteinVolume: calculating molecular van der Waals and void volumes in proteins BMC Bioinf 16:1-6

Gallicchio E, Kubo M, Levy RM (2000) Enthalpy− entropy and cavity decomposition of alkane hydration free energies: Numerical results and implications for theories of hydrophobic solvation J Phys Chem B 104:6271-6285

Giambaşu GM, Gebala MK, Panteva MT, Luchko T, Case DA, York DM (2015) Competitive interaction of monovalent cations with DNA from 3D-RISM Nucleic Acids Res 43:8405-8415

Giambaşu GM, Luchko T, Herschlag D, York DM, Case DA (2014) Ion counting from explicit-solvent simulations and 3D-RISM Biophys J 106:883-894

Gomes TC, Skaf MS (2012) Cellulose-Builder: A toolkit for building crystalline structures of cellulose J Comput Chem 33:1338-1346

Gusarov S, Pujari BS, Kovalenko A (2012) Efficient treatment of solvation shells in 3D molecular theory of solvation. J Comput Chem 33:1478-1494

Huh E, Yang J-H, Lee C-H, Ahn I-S, Mhin BJ (2020) Thermodynamic analysis of cellulose complex in NaOH–urea solution using reference interaction site model Cellulose 27:6767-6775

Imai T (2007a) Molecular theory of partial molar volume and its applications to biomolecular systems. Condens Matter Phys 10:343-361

Imai T, Ohyama S, Kovalenko A, Hirata F (2007b) Theoretical study of the partial molar volume change associated with the pressure-induced structural transition of ubiquitin. Protein Sci 16: 1927-1933

Jakalian A, Bush BL, Jack DB, Bayly CI (2000) Fast, efficient generation of high-quality atomic charges. AM1-BCC model: I. Method. J Comput Chem 21:132-146

Jakalian A, Jack DB, Bayly CI (2002) Fast, efficient generation of high-quality atomic charges. AM1-BCC model: II. Parameterization and validation. J Comput Chem 23: 1623-1641

Kovalenko A (2013) Multiscale modeling of solvation in chemical and biological nanosystems and in nanoporous materials. Pure Appl Chem 85:159-199

Kovalenko A (2017) Multiscale modeling of solvation. In: Breitkopf C, Swider-Lyons K (eds) Springer handbook of electrochemical energy. Springer, Heidelberg, pp 95–139

410 Kovalenko A, Gusarov S (2018) Multiscale methods framework: self-consistent coupling of
411 molecular theory of solvation with quantum chemistry, molecular simulations, and dissipative
412 particle dynamics. Phys Chem Chem Phys 20:2947-2969
413 Krüger P, Schnell SK, Bedeaux D, Kjelstrup S, Vlugt TJ, Simon J-M (2013) Kirkwood–Buff
414 integrals for finite volumes. J Phys Chem Lett 4:235-238
415 Lazaridis T (2000) Solvent reorganization energy and entropy in hydrophobic hydration. J Phys
416 Chem B 104:4964-4979
417 Lee B (1983) Partial molar volume from the hard-sphere mixture model. J Phys Chem 87:112-118
418 Misin M (2017) Can approximate integral equation theories accurately predict solvation
419 thermodynamics? Ph.D. thesis, University of Strathclyde. arXiv:1704.05246.
420 Misin M, Vainikka PA, Fedorov MV, Palmer DS (2016) Salting-out effects by pressure-corrected
421 3D-RISM. J Chem Phys 145:194501
422 Nicol TW, Isobe N, Clark JH, Shimizu S (2017) Statistical thermodynamics unveils the dissolution
423 mechanism of cellobiose Phys Chem Chem Phys 19:23106-23112
424 Patel N, Dubins DN, Pomes R, Chalikian TV (2011) Parsing partial molar volumes of small
425 molecules: A molecular dynamics study. J Chem Phys B 115:4856-4862
426 Sergiievskyi VP, Jeanmairet G, Levesque M, Borgis D (2014) Fast computation of solvation free
427 energies with molecular density functional theory: Thermodynamic-ensemble partial molar
428 volume corrections. J Phys Chem Lett 5:1935-1942
429 Shimizu S (2004) Estimating hydration changes upon biomolecular reactions from osmotic stress,
430 high pressure, and preferential hydration experiments. Proc Natl Acad Sci U S A 101:1195-1199
431 Shimizu S, Booth JJ, Abbott S (2013) Hydrotropy: binding models vs. statistical thermodynamics.
432 Phys Chem Chem Phys 15:20625-20632
433 Wang S, Lyu K, Sun P, Lu A, Liu M, Zhuang L, Zhang L (2017) Influence of cation on the
434 cellulose dissolution investigated by MD simulation and experiments. Cellulose 24:4641-4651
435 Wernersson E, Stenqvist B, Lund M (2015) The mechanism of cellulose solubilization by urea
436 studied by molecular simulation. Cellulose 22:991-1001
437 Xiong B, Zhao P, Cai P, Zhang L, Hu K, Cheng G (2013) NMR spectroscopic studies on the
438 mechanism of cellulose dissolution in alkali solutions. Cellulose 20:613-621

Figures

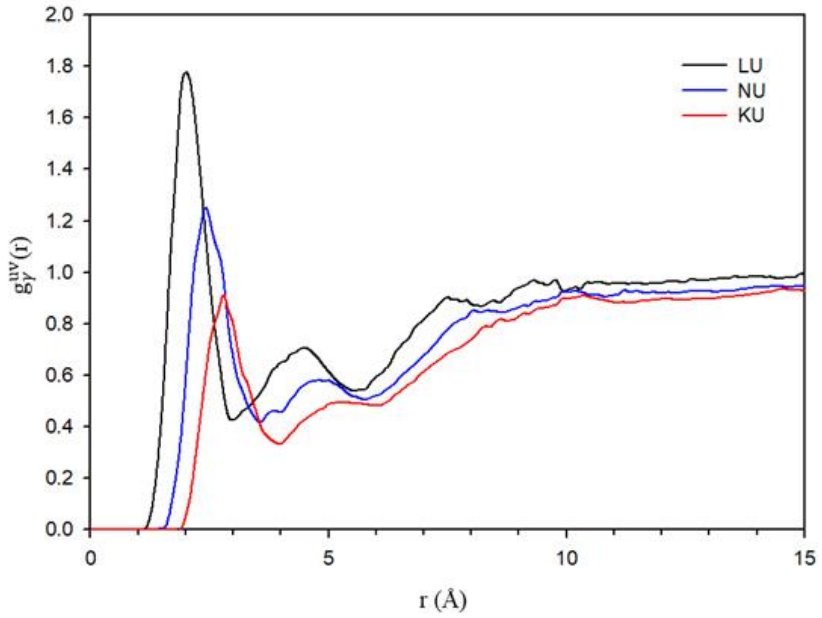

Fig. 1 Pair distribution function ($g_\gamma^{uv}(r)$) of Li^+, Na^+ and K^+ to the O2 atoms of cellulose in solvents LU, NU, and KU. Refer to Fig. 2 of Huh et al. (Huh et al. 2020) for the O2 atoms of cellulose.

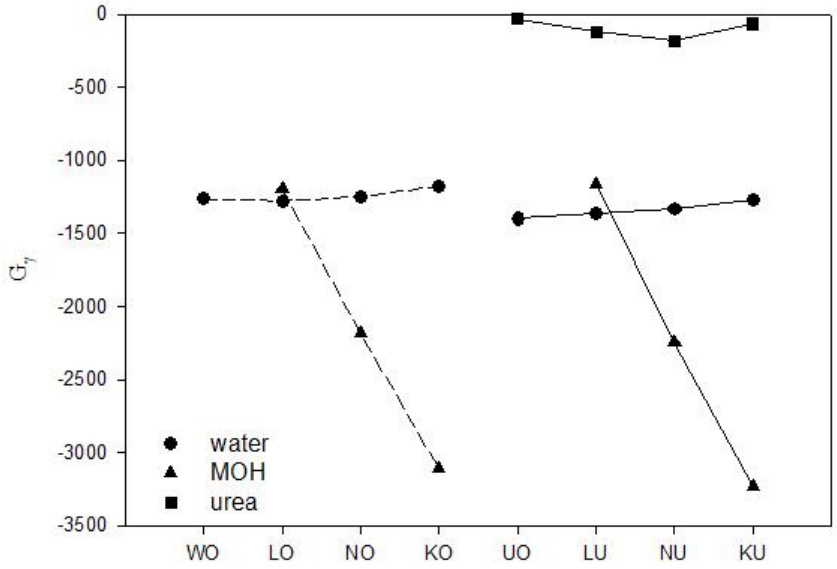

Fig. 2 Kirkwood Buff Integral (G_γ) for a solvent species γ in 8 different solvents: (●) for water; (▲) for an alkali metal hydroxide (MOH); and (■) for urea. The unit of G_γ is Å^3 per cellulose molecule.

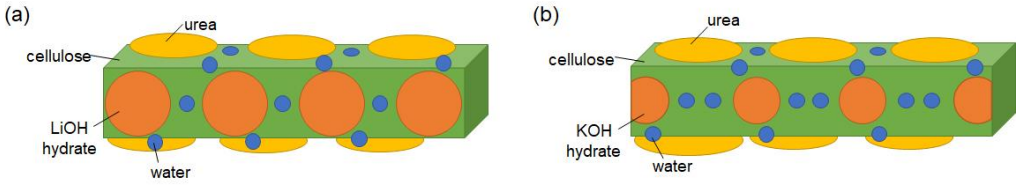

Fig. 3 Schematic depiction of solvent species around the single cellulose molecule in solvents LU (A) and KU (B). Urea (*yellow circle*) and hydrated MOH (*orange colored circle*) are positioned near the hydrophobic and hydrophilic parts of cellulose, respectively. Note the differences in the numbers of MOH and water molecules (*blue circle*) between (A) and (B).

Table

Table 1. Excess number of solvent species γ (N_{γ}^{excess}) in various solvents.

solvent	Water	LiOH/NaOH/KOH	Urea
LU	–0.8	0.0	1.4
NU	0.4	–1.2	1.3
KU	2.4	–2.3	1.5
UO	–1.2		1.5

457 **Table 2.** Cavity volume (V_C), interaction volume (V_I), ideal fluctuation volume (V_{id}), and partial
458 molar volume ($\bar{V}$) of cellulose in solvents LU, NU, and KU [a]

solvent	V_C	V_I	V_{id}	$\bar{V}$	V_T [b]
LU	1335.0	–57.5	1.5	1278.8	161.7
NU	1339.4	–57.4	1.4	1283.4	166.1
KU	1347.1	–50.5	1.3	1297.7	173.8
UO [c]	1360.5	–48.7	1.8	1313.6	187.2

459 [a] $\bar{V} = V_C + V_I + V_{id}$. The unit is Å^3 per cellulose molecule.
460 [b] V_T is the thermal volume and calculated from $V_T = V_C - V_M$ where $V_M = 1173.3$ Å^3.
461 [c] Data in solvent UO are given for comparison.
462

463 **Table 3.** $V_{C,\gamma}$ and $V_{I,\gamma}$, components of V_C and V_I for solvent species γ [a]

solvent	$V_{C,water}$	$V_{C,MOH}$	$V_{C,urea}$	$V_{I,water}$	$V_{I,MOH}$	$V_{I,urea}$
LU	1234.7	16.4	84.0	–50.9	–3.5	–3.4
NU	1210.1	45.0	84.3	–49.9	–4.0	–3.4
KU	1186.6	75.1	85.4	–43.4	–4.2	–3.0
UO [b]	1277.7		82.8	–45.9		–2.8

464 [a] The unit is Å^3 per cellulose molecule. Values of V_C and V_I are shown in Table 2.

465 [b] Data in solvent UO are given for comparison.

466

Table 4. Solvation energy and solvation entropy of cellulose in solvents LU, NU, and KU at 261 K [a]

solvent	ΔE	E^{uv}	ΔE^{R} $(\approx T\Delta S^{R})$	$T\Delta S$	$T\Delta S^{uv}$
LU	–1672.4	–481.4 (–411.8) [–49.7]	–1191.0 (–1086.0) [–101.2]	–1709.8	–518.7 (–460.6) [-29.3]
NU	–1600.9	–470.9 (–415.0) [–36.1]	–1130.0 (–1067.3) [–61.7]	–1658.8	–528.8 (–471.2) [–27.9]
KU	–1537.9	-450.7 (–403.9) [–26.9]	–1087.2 (–1054.7) [–33.2]	–1631.5	–544.3 (–482.7) [–30.2]
UO [b]	–142.2	–306.6 (–287.4)	164.3 (159.7)	–231.9	–67.6 (–51.0)

[a] $\Delta E = E^{uv} + \Delta E^{R}$ and $T\Delta S = T\Delta S^{uv} + T\Delta S^{R}$. The superscripts uv and R denote solute-solvent interaction and solvent reorganization (solvent-solvent interaction), respectively. Numbers in round and square brackets indicate the contributions of water and MOHs, respectively. The unit of energy is kcal per mole of cellulose.

[b] Data in solvent UO are given for comparison.

475 **Table 5.** Effect of MOHs and urea on the direct solvation energy (uv) and the solvent
476 reorganization energy (R) [a]

MOH	ΔE^{uv}_{MOH-WO}	ΔE^{uv}_{MOH-UO}	$\Delta\Delta E^{R}_{MOH-WO}$	$\Delta\Delta E^{R}_{MOH-UO}$
LiOH	–17.2	–174.8	–3.8	–1355.3
NaOH	–4.9	–164.3	16.5	–1294.3
KOH	–3.7	-144.1	28.2	–1251.5

477 [a] These energies are calculated at 261 K and their unit is kcal per mole of cellulose. The definitions
478 of ΔE^{uv}_{MOH-WO}, ΔE^{uv}_{MOH-UO}, $\Delta\Delta E^{R}_{MOH-WO}$, and $\Delta\Delta E^{R}_{MOH-UO}$ are shown in Eqs. (8)-(11).
479

480 **Table 6.** Chemical potentials of cellulose solvation without ($\Delta\mu$) and with ($\Delta\mu_{PC+}$), the advanced
481 pressure correction (PC+) in solvents LU, NU, and KU at 261 K [a]

MOH	$\Delta\mu$	$\Delta\mu_{PC+}$
LU	37.4	–193.8
NU	57.9	–188.6
KU	93.7	-178.4
UO [b]	89.7	–107.9

482 [a] The unit of energy is kcal per mole of cellulose.
483 [b] Data in solvent UO are given for comparison.

Figures

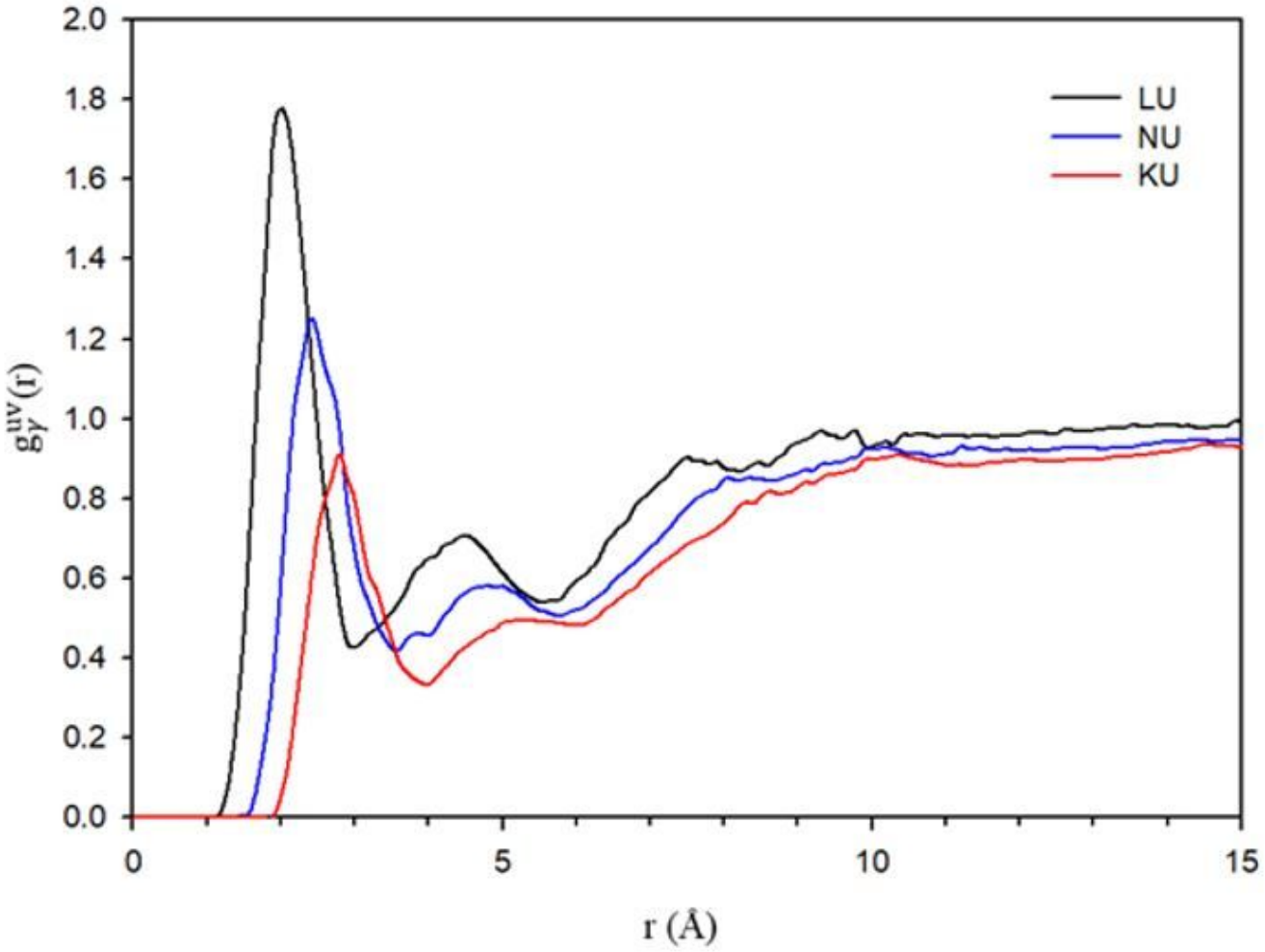

Figure 1

Pair distribution function (g_γ^uv (r)) of Li+, Na+ and K+ to the O2 atoms of cellulose in solvents LU, NU, and KU. Refer to Fig. 2 of Huh et al. (Huh et al. 2020) for the O2 atoms of cellulose.

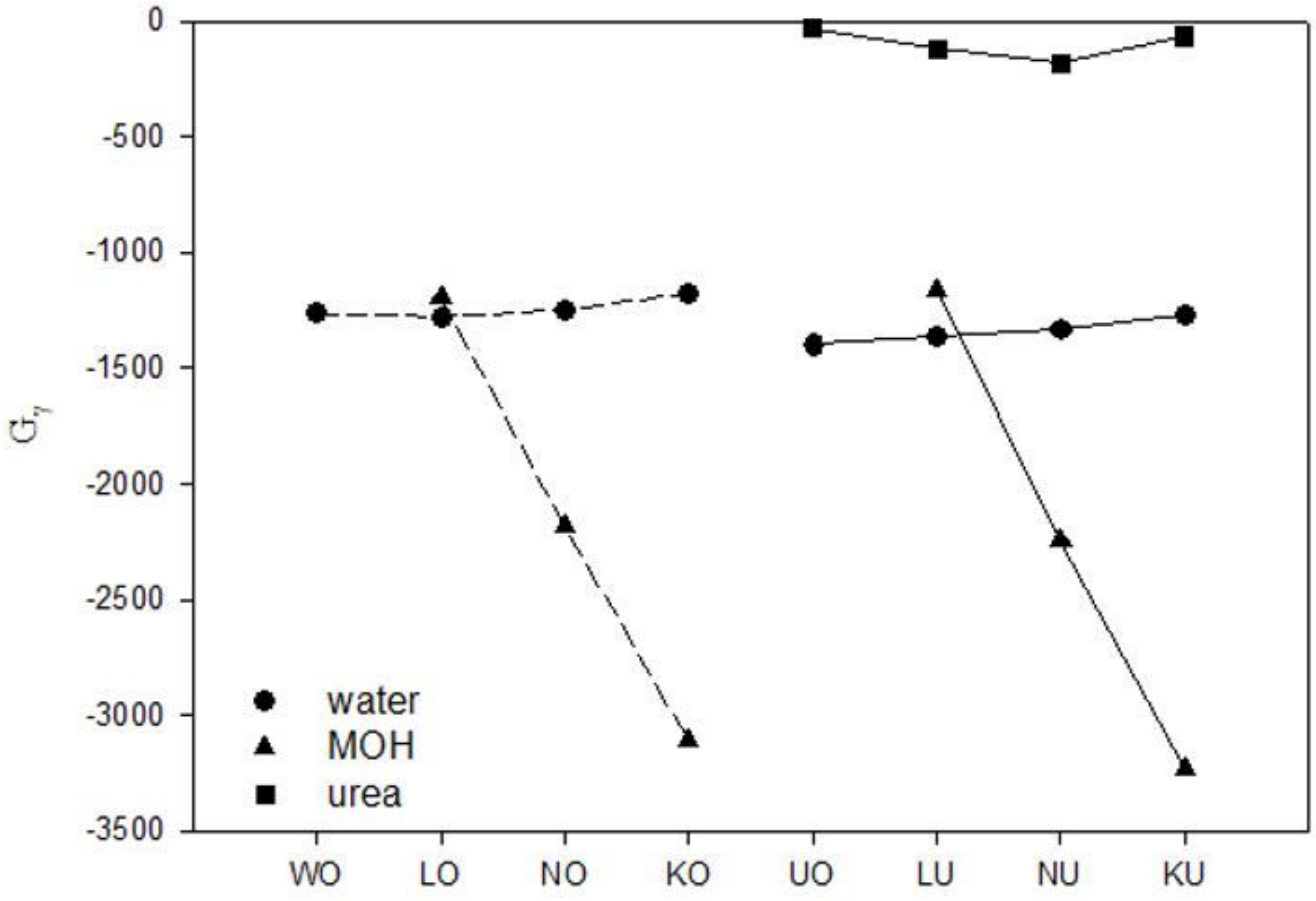

Figure 2

Kirkwood Buff Integral (G_γ) for a solvent species γ in 8 different solvents: (▯) for water; (▯) for an alkali metal hydroxide (MOH); and (▯) for urea. The unit of G_γ is Å3 per cellulose molecule.

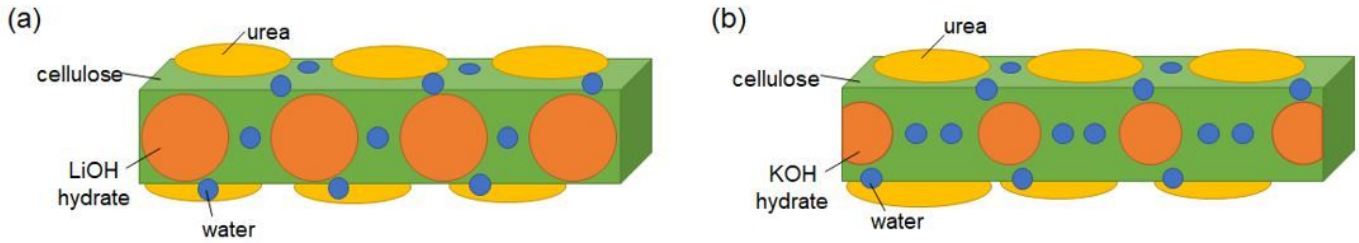

Figure 3

Schematic depiction of solvent species around the single cellulose molecule in solvents LU (A) and KU (B). Urea (yellow circle) and hydrated MOH (orange colored circle) are positioned near the hydrophobic

and hydrophilic parts of cellulose, respectively. Note the differences in the numbers of MOH and water molecules (blue circle) between (A) and (B).

Supplementary Files

This is a list of supplementary files associated with this preprint. Click to download.

- SupplementaryInformation.docx